Computer Modelling of Reaction-Diffusion Processes in Scanning Electrochemical Microscopy and in Cell Spheroids

Rokas Astrauskas

Scientific supervisor: prof. habil. dr. Feliksas Ivanauskas

Faculty of Mathematics and Informatics
Institute of Computer Science
Vilnius University

Vilnius Tech, September 2021

Vilnius University

Table of contents

Table of Contents

Outline of the study

- The goal is to develop mathematical and computational models of reaction-diffusion processes in scanning electrochemical microscopy(SECM).

- SECM is modelled by the system of 8 nonlinear reaction-diffusion equations, which are solved numerically.

- Research was carried in collaboration with VU CHGF chemists, led by prof. A. Ramanavičius.

Scanning Electrochemical Microscopy

Scanning electrochemical microscopy (SECM) is an electrochemical method, based on measurements with the ultramicroelectrode (UME), which is scanning 3D space around active surface.

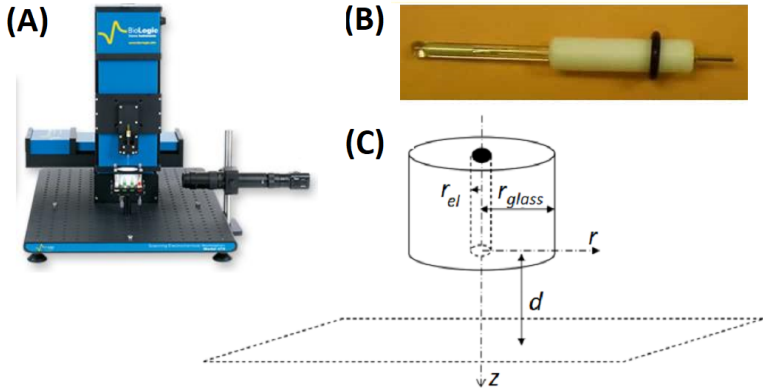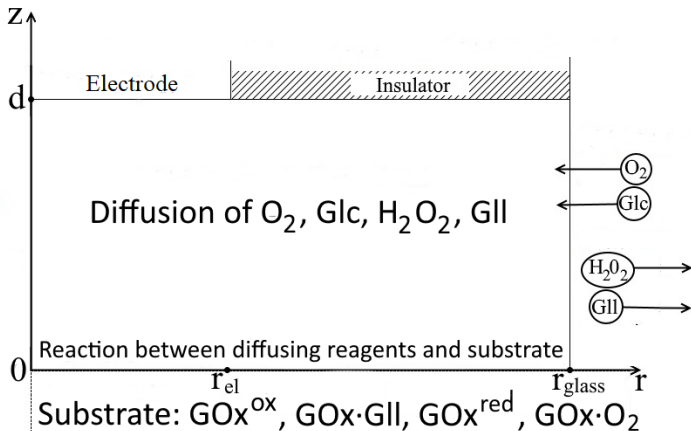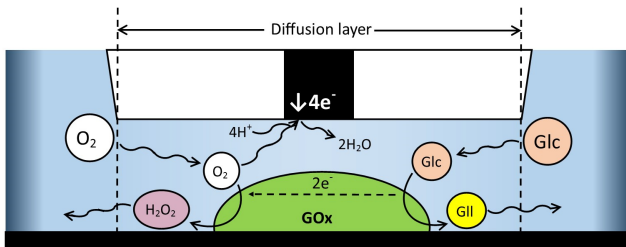
Figure: (A) ic-SECM470 from BioLogic. (B) PS108 platinum ultramicroelectrode (UME). (C) Scheme of probe and surface.

Scheme of SECM

3D domain is transformed into rectangular under central symmetry assumption. Cylindrical coordinates are used.

Redox-competition mode(RC-SECM)(1)

Chemical reactions on the enzyme-modified surface.

$$\text{GOx}^{\text{ox}} + \text{Glc} \underset{k_{-1}}{\overset{k_1}{\rightleftharpoons}} \text{GOx} \cdot \text{Glc} \overset{k_2}{\longrightarrow} \text{GOx}^{\text{re}} + \text{Gll}$$

$$\text{GOx}^{\text{re}} + \text{O}_2 \underset{k_{-3}}{\overset{k_3}{\rightleftharpoons}} \text{GOx} \cdot \text{O}_2$$

$$\text{GOx} \cdot \text{O}_2 \underset{k_{-4}}{\overset{k_4}{\rightleftharpoons}} \text{GOx}^{\text{ox}} + \text{H}_2\text{O}_2$$
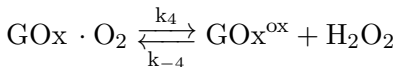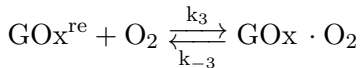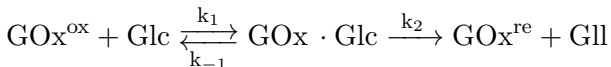
Redox-competition mode(2)

O_2 consumption on the UME surface, which is competing with enzymatic reactions

$$O_2 + 4\,e^- + 4\,H^+ \longrightarrow 2\,H_2O$$

Diffusion equations

Diffusion processes are expressed

$$\frac{\partial C_{O_2}}{\partial t} = D_{O_2} \, \Delta C_{O_2},$$

$$\frac{\partial C_{Glc}}{\partial t} = D_{Glc} \, \Delta C_{Glc},$$

$$\frac{\partial C_{H_2O_2}}{\partial t} = D_{H_2O_2} \, \Delta C_{H_2O_2},$$

$$\frac{\partial C_{Gll}}{\partial t} = D_{Gll} \, \Delta C_{Gll},$$

$$\text{for } 0 < t \leq T, \ 0 < z < d, \ 0 < r < r_{glass},$$

where Δ is Laplace operator with cylindrical symmetry

$$\Delta C = \frac{1}{r} \frac{\partial}{\partial r} \left(r \frac{\partial C}{\partial r} \right) + \frac{\partial^2 C}{\partial z^2}.$$

Reaction equations

Reactions equations for non-diffusing reagents on the surface $z = 0$ are

$$\frac{\partial C_{GOx^{ox}}}{\partial t} = -k_1 C_{GOx^{ox}} C_{Glc} + k_{-1} C_{GOx \cdot Gll} + k_4 C_{GOx \cdot O_2} -$$
$$- k_{-4} C_{GOx^{ox}} C_{H_2 O_2},$$

$$\frac{\partial C_{GOx \cdot Gll}}{\partial t} = k_1 C_{GOx^{ox}} C_{Glc} - (k_{-1} + k_2) C_{GOx \cdot Gll},$$

$$\frac{\partial C_{GOx^{red}}}{\partial t} = k_2 C_{GOx \cdot Gll} - k_3 C_{GOx^{red}} C_{O_2} + k_{-3} C_{GOx \cdot O_2},$$

$$\frac{\partial C_{GOx \cdot O_2}}{\partial t} = k_3 C_{GOx^{red}} C_{O_2} - k_{-3} C_{GOx \cdot O_2} - k_4 C_{GOx \cdot O_2} +$$
$$+ k_{-4} C_{GOx^{ox}} C_{H_2 O_2},$$

$$\textit{for } 0 < t \leq T, \ 0 < r < r_{glass}.$$

Initial-boundary conditions (1)

Only initial conditions are required for reaction equations

$$C_{GOx^{ox}} = 2.114 \ mol/m^2, \quad C_{GOx \cdot GlI} = C_{GOx^{red}} = C_{GOx \cdot O_2} = 0,$$
$$for \ t = 0, \ 0 < r < r_{glass}.$$

For diffusion equations initial conditions are

$$C_{O_2} = 253 \ \mu M, \quad C_{Glc} = C_{H_2O_2} = C_{GlI} = 0,$$
$$for \ t = 0, \ 0 < z < d, \ 0 < r < r_{glass},$$

and boundary conditions ...

Initial-boundary conditions (2)

Nonlinear boundary conditions on the surface $z = 0$ are derived from chemical reactions between diffusing reagents and substrate:

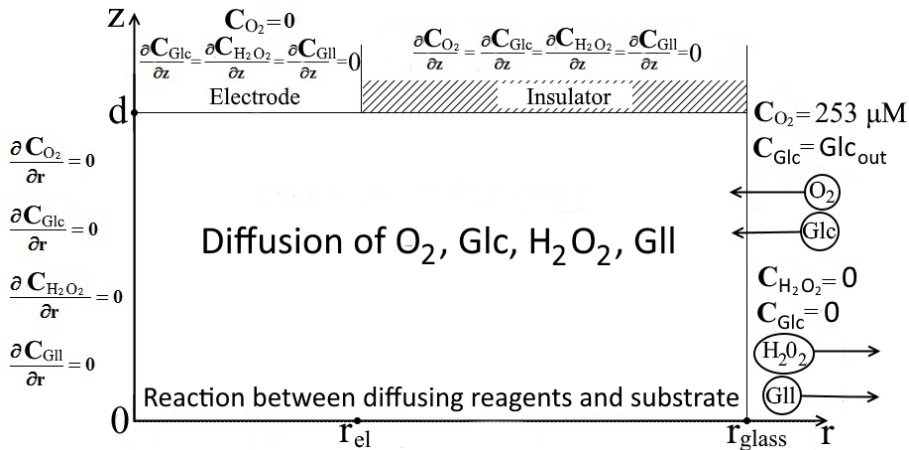$$D_{O_2}\frac{\partial C_{O_2}}{\partial z} = k_3 C_{GOx^{red}} C_{O_2} - k_{-3} C_{GOx \cdot O_2},$$

$$D_{Glc}\frac{\partial C_{Glc}}{\partial z} = k_1 C_{GOx^{ox}} C_{Glc} - k_{-1} C_{GOx \cdot Gll},$$

$$D_{H_2O_2}\frac{\partial C_{H_2O_2}}{\partial z} = -k_4 C_{GOx \cdot O_2} + k_{-4} C_{GOx^{ox}} C_{H_2O_2},$$

$$D_{Gll}\frac{\partial C_{Gll}}{\partial z} = k_2 C_{GOx \cdot Gll}, \quad \text{for } 0 < t \leq T, \ z = 0, \ 0 < r < r_{glass}.$$

Initial-boundary conditions (3)

All other boundary conditions are presented on the figure:

Non-uniform mesh(1)

Non-uniform spatial mesh is used with contractions around

- the surface of electrode $z = d$,
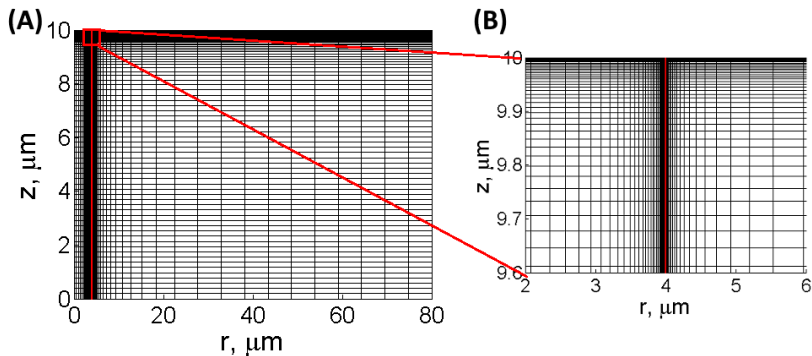- the junction between electrode and isolator $r = r_{el}$.

Figure: (A) full mesh, (B) Zoomed part of the mesh. Red line – the junction between electrode and isolator

Non-uniform mesh(2)

Computer experiments show that even small 50×50 non-uniform mesh works well compared with spatially uniform mesh.
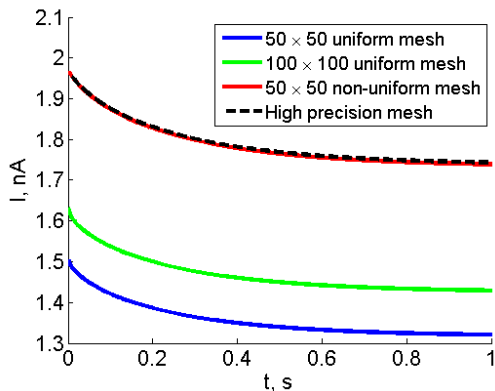

Figure: model parameters: $r_{el} = 5\mu m$, $r_{glass} = 50\mu m$, $d = 10\mu m$

Timestep

Temporal mesh is also non-uniform and timestep tau_k is set to

$$\tau_k = 0.0001, \quad for\ t < 1\ s,$$
$$\tau_k = 0.001, \quad for\ 1\ s \le t < 2\ s,$$
$$\tau_k = 0.01, \quad for\ 2\ s \le t < T$$

The size of timestep grid ~ 13000 depending on T.

Solving diffusion equations(1)

Alternating-direction implicit (ADI) finite difference method (FDM) is used to solve 4 diffusion equations.

Motivation for ADI algorithm:

- Approximation error is $\mathcal{O}(\tau^2 + h^2)$. Order 2 is considered highly accurate.
- Unconditional stability, i.e. τ does not depend on spatial step h.

Solving diffusion equations(2)

For example, discretization while solving to r-direction:

$$\frac{\overline{U}_{i,j} - U_{i,j}^k}{0.5\tau_k} = \frac{D}{r_j l_{j+0.5}} \left(r_{j+0.5} \frac{\overline{U}_{i,j+1} - \overline{U}_{i,j}}{l_{j+1}} - r_{j-0.5} \frac{\overline{U}_{i,j} - \overline{U}_{i,j-1}}{l_j} \right) +$$

$$+ \frac{D}{h_{i+0.5}} \left(\frac{U_{i+1,j}^k - U_{i,j}^k}{h_{i+1}} - \frac{U_{i,j}^k - U_{i-1,j}^k}{h_i} \right),$$

$$j = 1, \ldots, N_2 - 1,$$

where U^k – known value of diffusing reagent at previous timestep, $\overline{U}$ – unknown *mid-step* value.
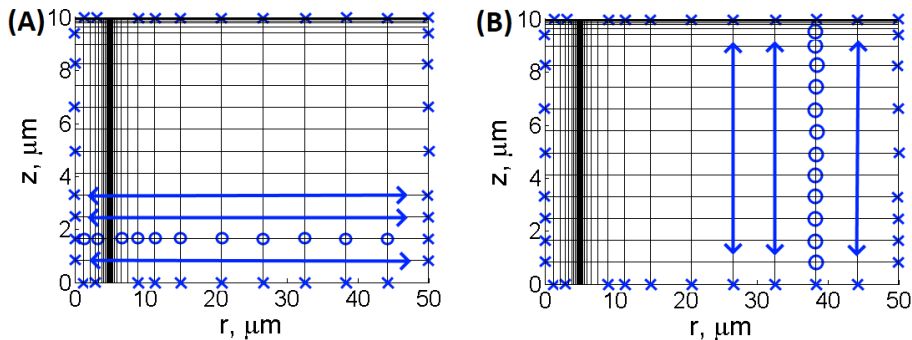
Solving diffusion equations(3)

Figure: Solution to (A) *r*-direction, (B) *z*-direction. Blue circles – inner points of the domain, blue crosses – boundary points.

Values at boundary points are approximated separately using boundary condition and differential eq.

System of linear equations

Systems of linear equations $AU = B$ are derived from approximations at each line.

The matrix A is always tridiagonal

$$A = \begin{pmatrix} b_0 & c_0 & 0 & \dots & 0 \\ a_1 & b_1 & c_1 & \dots & 0 \\ 0 & a_2 & b_2 & \dots & 0 \\ \vdots & & & \ddots & \vdots \\ 0 & 0 & 0 & \dots & b_N \end{pmatrix}$$

and are solved by efficient Thomas algorithm in $\mathcal{O}(N)$ time.

Nonlinear boundary condition(1)

Special case while solving to z-direction is boundary condition at $z = 0$, because **nonlinear system** is formulated by approximating:

$$\frac{U_{0,j}^{k+1} - \overline{U}_{0,j}}{0.5\tau_k} = \frac{D}{r_j l_{j+0.5}} \left(r_{j+0.5} \frac{\overline{U}_{N_1,j+1} - \overline{U}_{N_1,j}}{l_{j+1}} - r_{j-0.5} \frac{\overline{U}_{N_1,j} - \overline{U}_{N_1,j-1}}{l_j} \right)$$
$$+ 2D \frac{U_{1,j}^{k+1} - U_{0,j}^{k+1}}{h_1^2} - \frac{2}{h_1} F_{\text{boundary}}(\mathbf{U}_{0,j}^{k+1}, \mathbf{V}_j^{k+1}),$$

where V - non-diffusing reagent, $F_{\text{boundary}}(\mathbf{U}, \mathbf{V})$ – functions from boundary condition at $z = 0$.

Nonlinear boundary condition(2)

Two solutions are provided for nonlinear system:

- Iterative algorithm. At each timestep couple of iterations of solving to r-direction, to z-direction and then reaction equations are repeated until $U_{O_2}^{(iter)}$ converges.
- Simple linearization is used

$$\frac{U_{0,j}^{k+1} - \overline{U}_{0,j}}{0.5\tau_k} = \frac{D}{r_j l_{j+0.5}} \left(r_{j+0.5} \frac{\overline{U}_{N_1,j+1} - \overline{U}_{N_1,j}}{l_{j+1}} - r_{j-0.5} \frac{\overline{U}_{N_1,j} - \overline{U}_{N_1,j-1}}{l_j} \right)$$
$$+ 2D \frac{U_{1,j}^{k+1} - U_{0,j}^{k+1}}{h_1^2} - \frac{2}{h_1} F_{\text{boundary}}(\mathbf{U}_{0,j}^k, \mathbf{V}_j^k),$$

because it has been determined that 2nd iteration is very close to the 1st according to performed computer simulations.

Solving reaction equations(1)

System of ODEs for non-diffusing reagents V is approximated by implicit Crank-Nicolson scheme:

$$\frac{V_{GOx^{ox},j}^{k+1} - V_{GOx^{ox},j}^{k}}{\tau} = -k_1 \widehat{V}_{GOx^{ox},j} \widehat{U}_{Glc,0,j} + k_{-1} \widehat{V}_{GOx \cdot GlI,j} +$$
$$+ k_4 \widehat{V}_{GOx \cdot O_2} - k_{-4} \widehat{V}_{GOx^{ox},j} \widehat{U}_{H_2O_2,0,j},$$

$$\frac{V_{GOx \cdot GlI,j}^{k+1} - V_{GOx \cdot GlI,j}^{k}}{\tau} = k_1 \widehat{V}_{GOx^{ox},j} \widehat{U}_{Glc,0,j} - (k_{-1} + k_2) \widehat{V}_{GOx \cdot GlI,j},$$

$$\frac{V_{GOx^{red},j}^{k+1} - V_{GOx^{red},j}^{k}}{\tau} = k_2 \widehat{V}_{GOx \cdot GlI,j} - k_3 \widehat{V}_{GOx^{red},j} \widehat{U}_{O_2,0,j} +$$
$$+ k_{-3} \widehat{V}_{GOx \cdot O_2,j},$$

Solving reaction equations(2)

$$\frac{V_{GOx \cdot O_2, j}^{k+1} - V_{GOx \cdot O_2, j}^{k}}{\tau} = k_3 \widehat{V}_{GOx^{red}, j} \widehat{U}_{O_2, 0, j} - k_{-3} \widehat{V}_{GOx \cdot O_2, j} -$$

$$- k_4 \widehat{V}_{GOx \cdot O_2, j} + k_{-4} \widehat{V}_{GOx^{ox}, j} \widehat{U}_{H_2 O_2, 0, j},$$

$$j = 0, \ldots, N_2 - 1,$$

where $\widehat{U}_{0,j} = \left(U_{0,j}^{k} + U_{0,j}^{k+1} \right)/2$, $\widehat{V}_j = \left(V_j^{k} + V_j^{k+1} \right)/2$,
U^{k+1} – already calculated, V^{k+1} – unknown values.

At each index j easily solvable system of 4 linear equations is derived

$$A\mathbf{V}_j^{k+1} = B.$$

Programming details

Program code (~ 1000 lines for model $+ \sim 600$ for support functions) has been implemented using Python (Anaconda distribution) using libraries

- *numpy* – vectors, matrices, vectorized computing,
- *numba* – @jit decorator for optimized compiler,
- *multiprocessing* – parallelizing computations on MIF cluster.

MATLAB has also been used for

- initial program,
- data analysis and graphics.

Model verification: convergence to exact solution

Numerical solution converges to exact solution as mesh size increases
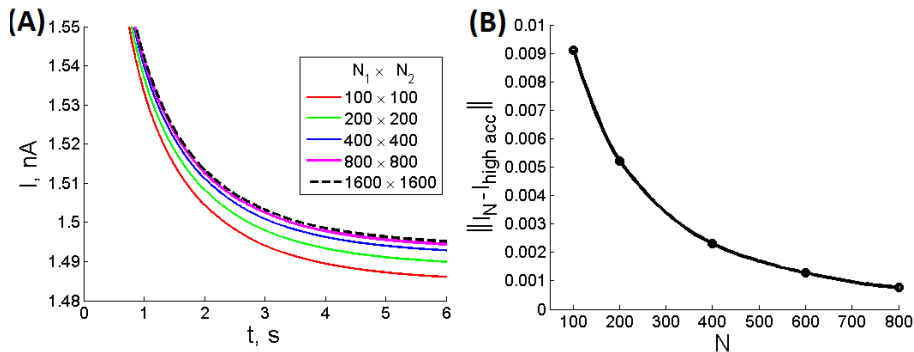
Figure: (A) Graph of electric currents, (B) errors between electric currents.

SECM electric current

Numerical solution for all 8 reagents are calculated, e.g. (A) O_2 and (B) Glc at the time T:

(A)

(B)
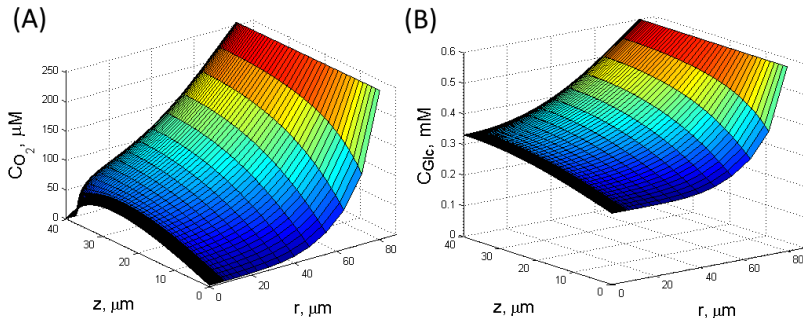
Results of chemical experiment are provided by electric current, which is measured by the electrode at position $z = 0$:

$$i(t) = 2\pi n F D_{O_2} \int_0^{r_{el}} \frac{\partial C_{O_2}}{\partial z}\bigg|_{z=d} r \, dr.$$

Comparison of simulations and chemical experiments

Results of computer simulations are compared with real SECM
experiments and good correspondence is achieved.
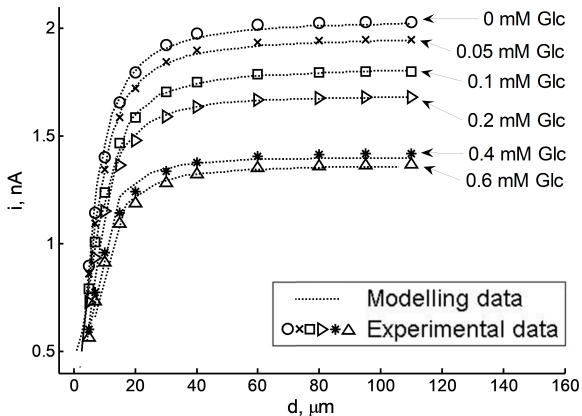
Figure: Electric current vs distance dependency.

Calculation of D_{O_2}

Formulae for O_2 diffusion coefficient is derived by fitting simulations data to the physical experiment:

$$D_{O_2} = 4.7 \cdot 10^{-10} + \frac{2.7 \cdot 10^{-10}}{Glc_{out} + 0.4}.$$
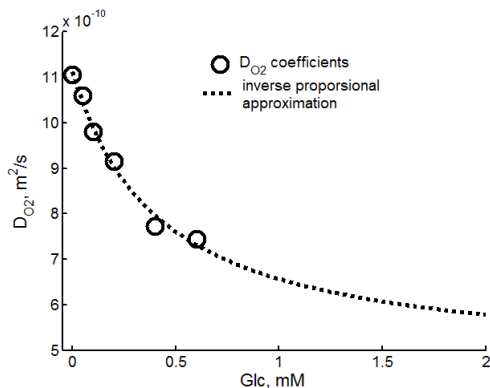
Conclusions

Summary of results

- Mathematical model of RC-SECM mode was presented for the first time in the literature.
- Using the model, it is possible to calculate
  - O_2 diffusion coefficients,
  - enzymatic reaction kinetics k_1, k_{-1}, etc.,
  - O_2 consumption rate.

Research was published in *F. Ivanauskas et al (2016). Modelling of scanning electrochemical microscopy at redox competition mode using diffusion and reaction equations. Electrochimica Acta.*

- Q1 (Electrochemistry) journal,
- 14 citations as of 2021.

Table of Contents

Vilnius
University

Outline of the study

- Study focuses on the precision of SECM measurements with 3 most frequent types of nonideal electrodes(UMEs): reccesed, outwarded (protruding), cone-shaped.
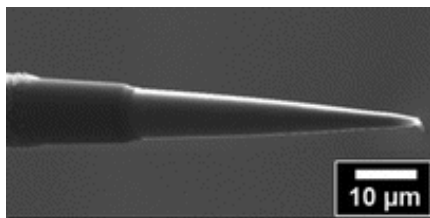

Figure: Example of non-standard electrode: cone-shaped nanoelectrode

- UMEs are mathematically modelled by diffusion equation in various non-standard (non-rectangular) domains.

- Measurement errors between experiments performed by perfect electrode and by defected UMEs are evaluated.
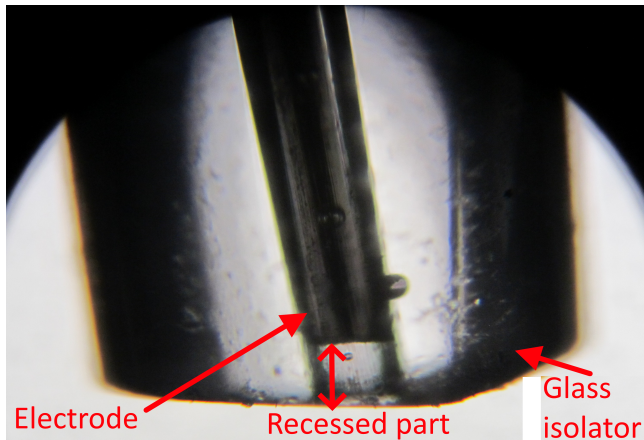
Motivation(1)

Figure: Image of the probe with recessed-UME. This equipment is used for physical experiment in our study.

Motivation(2)

Variations in UME geometry are caused by 2 major factors:

1 Deviation from an ideal shape of UME are hard to avoid due to sophisticated procedure of UME fabrication.

2 The geometry of the UME changes every time, when UME is
  - polished during cleaning,
  - accidentally damaged by touching the surface of interest.

Standard-plane-UME(1)

Rectangular domain is used to represent the geometry of standard-plane-UME.
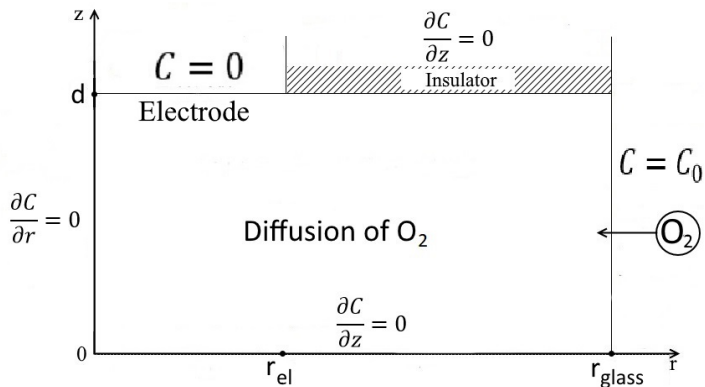
Standard-plane-UME(2)

Diffusion of O_2 is expressed by

$$\frac{\partial C}{\partial t} = D_{O_2}\left(\frac{\partial^2 C}{\partial r^2} + \frac{1}{r}\frac{\partial C}{\partial r} + \frac{\partial^2 C}{\partial z^2}\right),$$

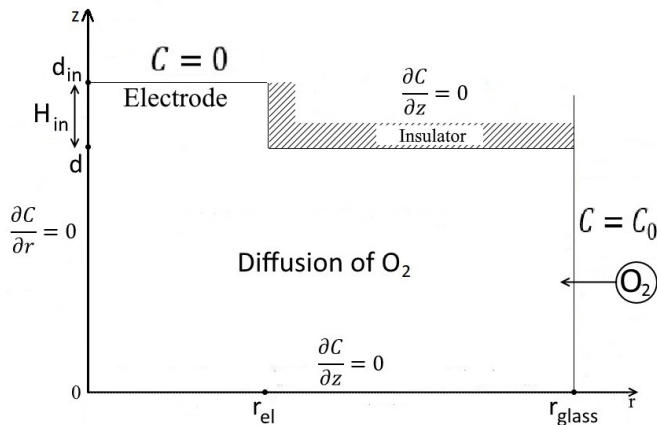$$\text{for } 0 < t \leq T,\ 0 < z < d,\ 0 < r < r_{glass}.$$

Initial condition is $C = 0.253\,\mu m$ for $0 < z < d,\ 0 < r < r_{glass}$.

All necessary boundary conditions were shown in figure.

Recessed-UME

UME's active (conducting) part is recessed by depth H_{in} into the insulating part of the electrode.
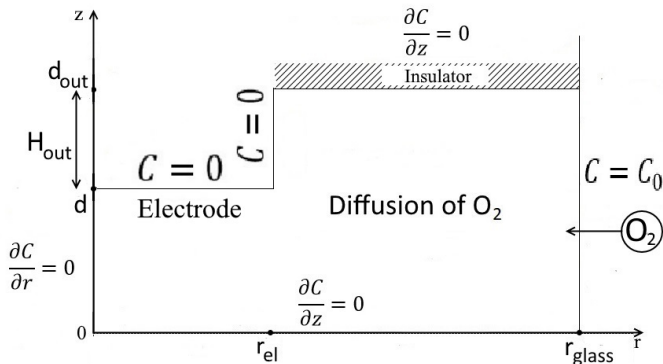
It may be caused by the damage to the wire of UME.

Outwarded-UME

Outwarded-UME is modelled as conducting cylinder bulging out of the insulating part of the UME into the diffusion layer.
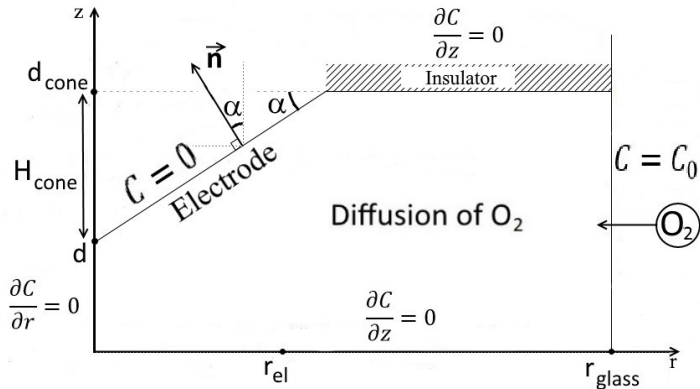Protrusion may be caused by the fractures of isolator glass which exposes the wire.

Cone-UME

The UME containing sharp sticking parts is modelled by a single
outwarded cone with one sharp tip.
Sharp surface of the electrode may be formed while cleaning UME with
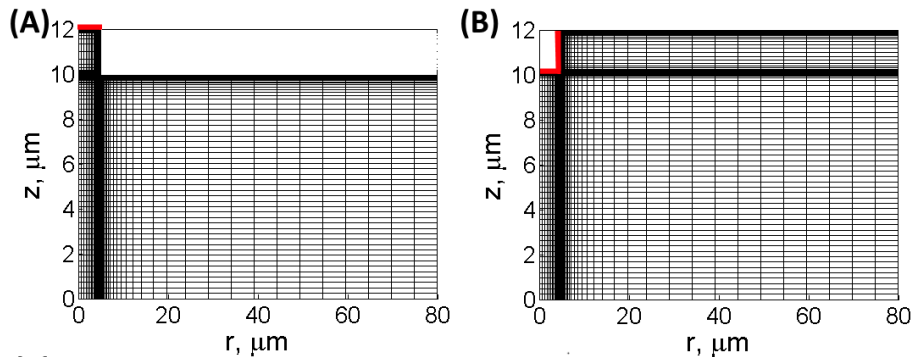sandpaper.

Mesh construction(1)

Figure: (A) recessed-UME, (B) outwarded-UME.
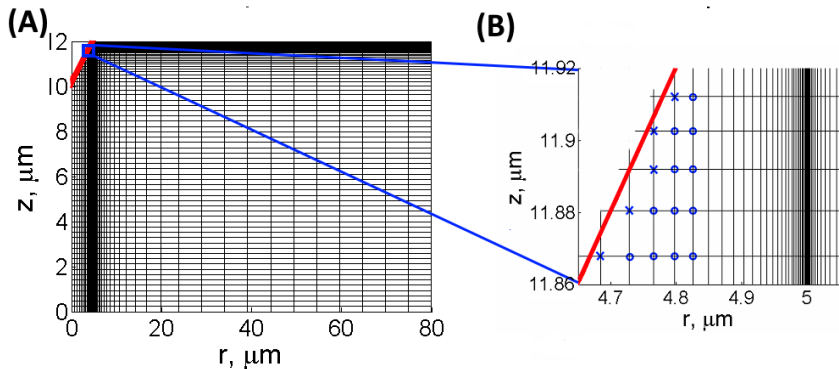
Mesh construction(2)

Figure: (A) cone-UME, (B) zoomed in part of cone-UME mesh.

Solving differential equation

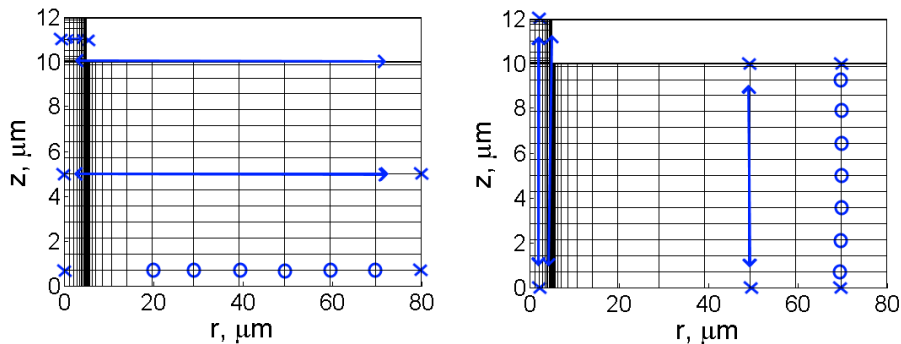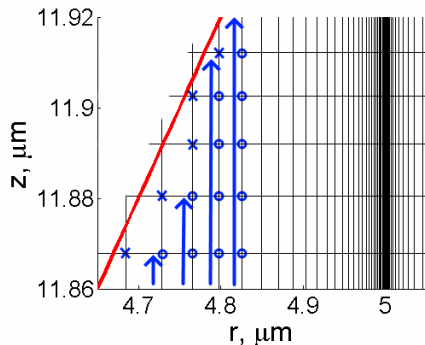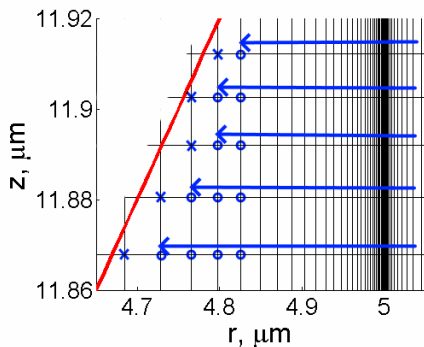ADI method is used to discretize and Thomas algorithm – to solve linear systems.

Figure: Example: Solution to both direction in reccesed-UME case

ADI method for Cone-UME

Numerical solution of cone-UME equation is complicated by boundary condition on the cone, which is *not parallel* to coordinates system, i.e. boundary line does not intersect with mesh points.

Programming details

- Algorithms were written in Python (500–700 lines of code for each model + extra functions).

- Due to high computational costs, parallel computations were performed on MIF cluster with *Lock* synchronization to ensure that processes do not override output.

- MATLAB was used for data work and plotting.

Model verification: convergence to standard-UME model

As cone height approaches 0, measured electric current converges to the current of standard-UME model:
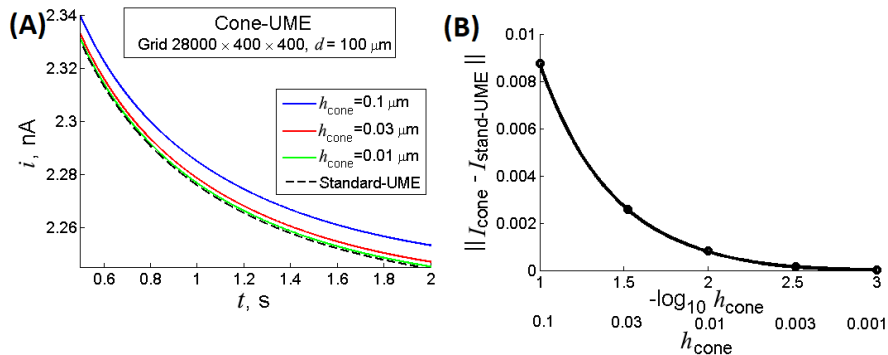

Figure: (A) electric currents, (B) errors.

Comparison of experiment and modelling data

Models of different geometries are compatible with real UMEs, which motivates the application of other models.
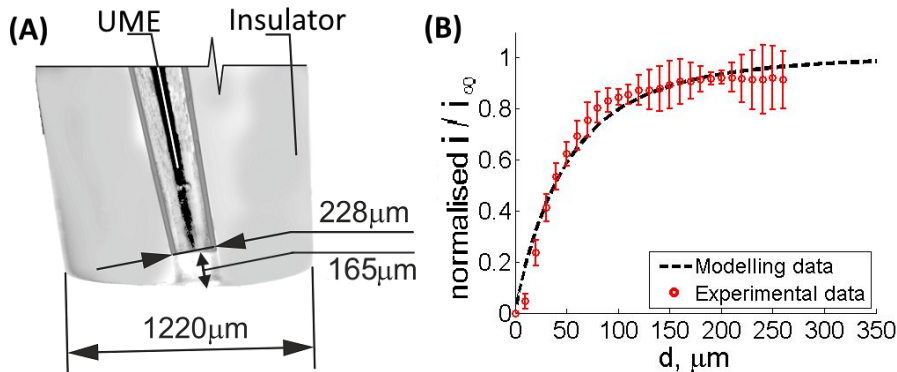

Figure: (A) Real-recessed-UME image. (B) Steady state current comparison for real UME and modelled recessed-UME. Error bars show standard deviation.

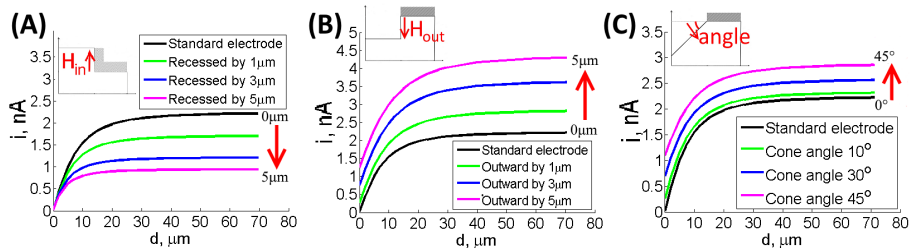# The influence of UME geometry on electric current

Figure: (A) recessed-UME, (B) outwarded-UME, (C) cone-UME.

Measurement errors for nonideal UMEs(1)
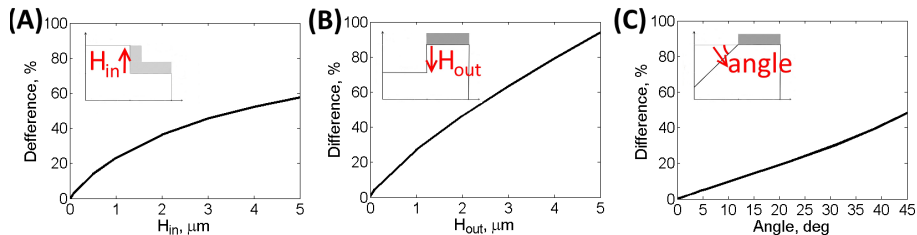
Figure: Differences between non-standard-UMEs and standard-plane-UME.

Measurement errors for nonideal UMEs(2)

Table: Dimensionless parameters of non-standard-UME geometries that provides following differences from standard-plane-UME.

Difference from standard-plane-UME	5 %	10 %	25 %	50 %
Recess depth H_{in}/r_{el}	0.034	0.075	0.225	0.745
Protrusion height H_{out}/r_{el}	0.027	0.064	0.186	0.438
Cone height H_{cone}/r_{el}	0.090	0.184	0.488	1.042

Conclusions

Summary of results

- Software tools were developed to evaluate measurement errors between experiments performed by standard perfect electrode and by nonideal UMEs.

- Outwarded-UME provides the highest measurement errors, whereas errors of reccesed-UME and cone-UME experiments are approximately 2 times lower with the same deviation from standard UME.

Research was published in *R. Astrauskas et al (2019). Mathematical Modelling of the Influence of Ultra-micro Electrode Geometry on Approach Curves Registered by Scanning Electrochemical Microscopy. Electroanalysis.*

- Q2 (Analytical Chemistry) journal,
- 7 citations as of 2021.

Table of Contents

Outline of the study

- The goal of the research was to develop novel model for fluorescent dyes uptake into spheroids and investigate the properties of penetration and accumulation.

- Mathematical models are based on
  - system of nonlinear reaction-diffusion equation,
  - diffusion equation with discontinous diffusion coefficient.

- Experimental data was provided by prof. R. Rotomskis group from National Cancel Institute.

Applications in medical physics

3D cell cultures are used as a platform for drug testing, but not all drugs can be investigated due to experimental limitations.

It would be useful to predict drug distribution into 3D cell cultures by using the data of already investigated molecules such as fluorescent dyes.
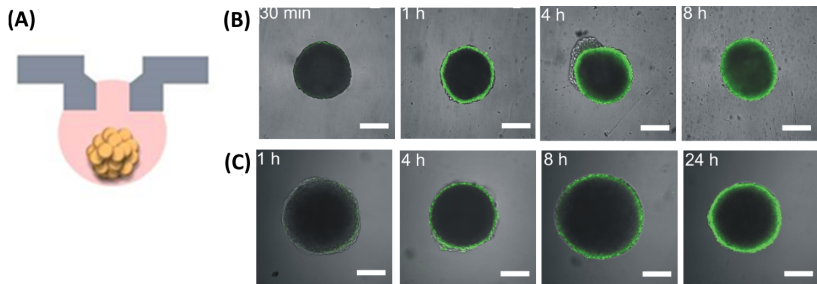
Figure: (A) 3D cellular spheroid, (B) R6G dye distribution in spheroids over time, (B) WGA distribution.

Schemes of models

3 models are provided

Ⓐ WGA (wheat agglutinin) model: WGA molecules diffusion is limited to cellular matrix, but molecules bind to cells.

Ⓑ R6G (rhodamine) model: R6G diffuses both through cells and matrix.

Ⓒ Rings model: rings of cells represent averaged cells and cellular matrix layer – material between the cells.

(A)
Bind
WGA
molecule
Binding
site

(B)
R6G
Cell
spheroid
Cells

(C)
d_{cell}
d_m
Cell
layer
Matrix
layer
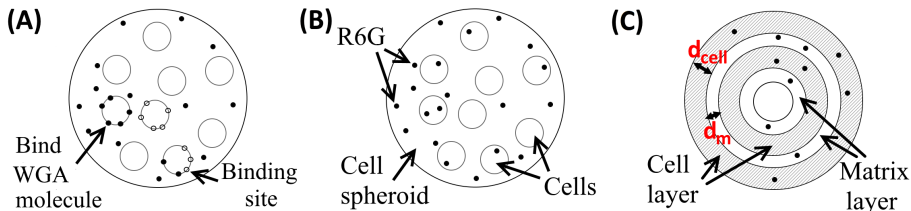
WGA migration model

Using spherical symmetry, WGA molecules diffusion and binding in 3D cell spheroids is expressed by:

$$\frac{\partial C_{out}}{\partial t} = D \frac{1}{r^2} \frac{\partial}{\partial r} \left(r^2 \frac{\partial C_{out}}{\partial r} \right) - k_{bind} k_{bind} (B_{max} - C_{bind}) C_{out},$$

$$0 < t \leq T, \ \ 0 < r < R,$$

where C_{out} – WGA molecules, which diffuse outside of cells, C_{bind} – WGA molecules which are bound to the cells.

The process of binding to cells:

$$\frac{\partial C_{bind}}{\partial t} = k_{bind} (B_{max} - C_{bind}) C_{out}, \quad 0 < t \leq T.$$

Initial-boundary conditions

Boundary conditions are necessary for C_{out}

$$C_{out}\big|_{r=R} = C_{outside},$$
$$\frac{\partial C_{out}}{\partial r}\bigg|_{r=0} = 0, \quad t > 0.$$

Initial conditions for both functions

$$C_{out}\big|_{t=0} = 0,$$
$$C_{bind}\big|_{t=0} = 0, \quad 0 \le r \le R.$$

Rhodamine migration model

Diffusion of R6G molecules in spheroids is modelled using equation and initial-boundary conditions:

$$\frac{\partial C}{\partial t} = D\frac{1}{r^2}\frac{\partial}{\partial r}\left(r^2\frac{\partial C}{\partial r}\right), \quad \text{for } 0 < t \leq T, \ 0 < r < R,$$

$$C\big|_{r=R} = C_{outside}, \quad t > 0,$$

$$\frac{\partial C}{\partial r}\bigg|_{r=0} = 0, \quad t > 0,$$

$$C\big|_{t=0} = 0, \quad 0 \leq r \leq R.$$

Ring model for R6G migration

Diffusion equation with non-constant diffusion coefficient is used:

$$\frac{\partial C}{\partial t} = \frac{1}{r^2}\frac{\partial}{\partial r}\left(r^2 D(r)\frac{\partial C}{\partial r}\right), \quad \textit{for } 0 < t \leq T, \ \ 0 < r < R,$$

$$C\big|_{r=R} = C_{outside}, \quad t > 0,$$

$$\frac{\partial C}{\partial r}\bigg|_{r=0} = 0, \quad t > 0,$$

$$C\big|_{t=0} = 0, \quad 0 \leq r \leq R,$$

where $D(r)$ – discontinuous diffusion coefficient

$$D(r) = \begin{cases} D_{cell}, & \text{if } r \in \text{cell layer,} \\ D_{matrix}, & \text{if } r \in \text{matrix layer.} \end{cases}$$

Approximating diffusion equation

2D uniform mesh is chosen consisting of 100 points in r direction and 240000 points in t direction.

Diffusion equation is discretized using Crank-Nicolson implicit scheme

$$\frac{U_i^{k+1} - U_i^k}{\tau} = D\left(\frac{\overline{U}_{i-1} - 2\overline{U}_i + \overline{U}_{i+1}}{h^2} + \frac{1}{r_i}\frac{\overline{U}_{i+1} - \overline{U}_{i-1}}{h}\right) -$$
$$- k_{bind}(B_{max} - \overline{V}_i)\overline{U}_i, \quad i = 1, \ldots, N-1,$$

where $\overline{U}_i = (U_i^{k+1} + U_i^k)/2$, $\overline{V}_i = (V_i^{k+1} + V_i^k)/2$,

$U \approx C_{out}$ and $V \approx C_{bind}$.

Approximating reaction equation

Reaction equation is discretized by midpoint method

$$\frac{V_i^{k+1} - V_i^k}{\tau} = k_{bind}\big(B_{max} - \overline{V}_i\big)\overline{U}_i, \quad i = 1, \ldots, N - 1,$$

Iterative solution to nonlinear system(1)

Nonlinear system of algebraic equations is derived from previous formulas

$$A\mathbf{U}^{k+1} = \widehat{A}\mathbf{U}^k + F(\mathbf{U}^{k+1}, \mathbf{U}^k),$$

where $\mathbf{U}^{k+1} = (U_0^{k+1}, \ldots, U_N^{k+1})$ – unknown values,
$\quad \mathbf{U}^k$ – values from previous timestep,
$\quad A$ and $\widehat{A}$ – matrices,
$\quad F$ – nonlinear part of the system, derived from the reaction term.

Iterative solution to nonlinear system(2)

This system is linearized by Picard's iterative process:

$$A\mathbf{U}^{(j+1)} = \widehat{A}\mathbf{U}^k + F(\mathbf{U}^{(j)}, \mathbf{U}^k), \quad j = 0, \ldots$$
$$\mathbf{U}^{(0)} = \mathbf{U}^k.$$

It is tridiagonal system, which is solved using Thomas algorithm at each iteration step.

Computer simulations have shown, that the process converges rapidly and no more than 4 iterations are required.

Comparing R6G experiments and simulations

Fig. (A): Diffusion coefficient in cellular matrix is calculated by fitting R6G model curve to experimental data.

Fig. (B): The model is validated by comparing fluorescence intensities in experimental and simulation data.
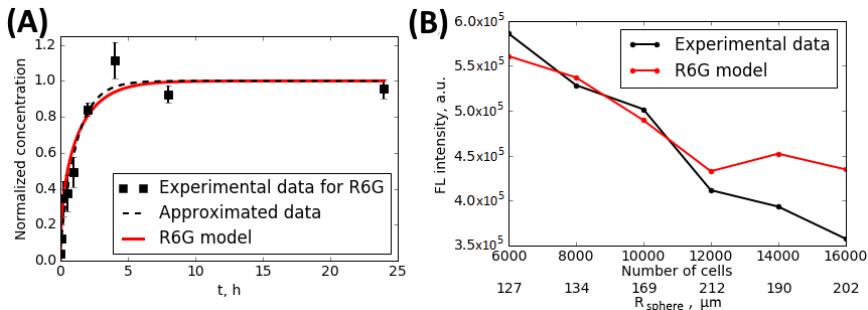

Figure: (A) R6G dye accumulated concentration vs time, (B) Accumulated fluorescence intensity vs spheroid size.

R6G accumulation dynamics

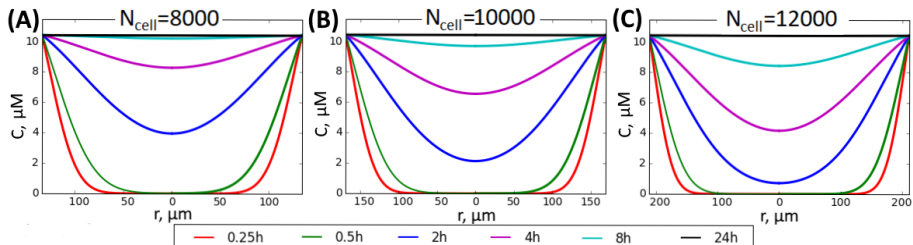Using the R6G migration model R6G dye accumulation inside spheroid is calculated

Figure: R6G concentration from the center to the sides of spheroid.

Nonlinear WGA model analysis

Using WGA model concentration in cellular matrix C_{out} and concentration of bound WGA molecules C_{bind} are computed.

Penetration rate for the smaller spheroid is faster than for the larger ones with the exception of largest spheroids due to changes in largerst spheroid formation.
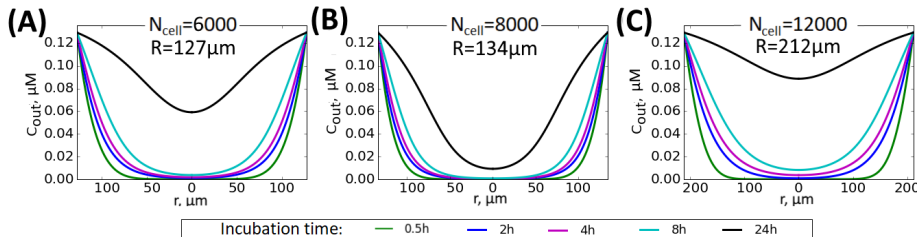

Figure: WGA dye concentration C_{out} in cellular matrix.

Conclusions

Main results of the study:

- Novel model for fluorescent dyes uptake into spheroids was developed.
- The properties of accumulation and penetration inside cells were investigated.
- Diffusion coefficient in the cellular matrix was calculated and it was determined that is about 4 times higher than in cells.

Research was published in *R. Astrauskas et al (2019). Modelling the uptake of fluorescent molecules into 3D cellular spheroids. Nonlinear Analysis: Modelling and Control.*

- Q2 (Applied Mathematics) journal.

Table of Contents

General conclusions(1)

1. The novel computer model of SECM is an appropriate tool for investigation of RC-SECM mode behaviour and determination of reaction and diffusion coefficients.

2. In particular, the diffusion coefficient of oxygen is inversely proportional to the concentration of glucose in the medium.

3. Mathematical models, which describe three most common non-standard geometries of ultramicroelectrode (UME), is an applicable technique to evaluate the difference from standard-UME in electric current measured by SECM electrodes.

General conclusions(2)

4. Outwarded-UME provides the highest measurement errors, whereas errors of reccesed-UME and cone-UME experiments are approximately 2 times lower with the same deviation from standard UME.

5. Using the model of R6G dye uptake into cellular spheroids, the diffusion coefficient in the cellular matrix has been calculated and it is about 4 times higher than the diffusion coefficient of cells.

6. By analysing accumulation dynamics into spheroids, time necessary to incubate the centre zone of the spheroid is calculated.